

Exploration of the Molecular Mechanism of *Curcuma aromatica* Salisb's Anticolorectal Cancer Activity via the Integrative Approach of Network Pharmacology and Experimental Validation

Zhi-Hui Yin, Wei-Hua Tan, and Yi-Ling Jiang*



Cite This: *ACS Omega* 2024, 9, 21426–21439



Read Online

ACCESS |

Metrics & More

Article Recommendations

Supporting Information

ABSTRACT: *Curcuma aromatica* Salisb (Cur), a well-known herbal medicine, has a wide spectrum of anti-inflammatory, anticarcinogenic, and antioxidant activities. However, the roles of its active compounds and potential mechanisms in colorectal cancer remain unknown. This research utilized network pharmacology and experimental validation to explore the possible mechanisms by which Cur protects against colorectal cancer. The active compounds of Cur and related genes for colorectal cancer were obtained from public databases. The DrugBank database was used to search for anticolorectal cancer drugs licensed through the FDA and their targets, and a “drug-component-target” relationship network was created using the Cytoscape program. The String database produced the PPI network. The ability of these active ingredients to bind to core targets was confirmed by molecular docking using AutoDock Vina. Cell and animal experiments were then carried out. A total of 274 targets were obtained from Cur, 49 of which were potential therapeutic targets. Four key targets, PTGS2, AKT1, TP53, and estrogen receptor 1 (ESR1), were screened via the PPI network and the FDA drug-target network. Molecular docking results revealed that Cur had strong binding abilities to these targets. In vivo and in vitro experiments demonstrated that Cur suppressed the development of colorectal cancer by regulating its targets (PTGS2, AKT1, TP53, and ESR1), which play crucial roles in promoting apoptosis and suppressing cell proliferation, migration, and invasion. Collectively, Cur protects against colorectal cancer by regulating the AKT1/PTGS2/ESR1 and P53 pathways, which lays the groundwork for further research and clinical applications of Cur in colorectal cancer therapy.



INTRODUCTION

The third most prevalent cancer, colorectal cancer, is one of the major reasons for cancer-associated deaths worldwide.^{1,2} Particularly in middle- and low-income nations, colorectal cancer incidence and mortality are rising quickly. The incidence of colorectal cancer is projected to increase by 60%, with an estimated 2.2 million new cases and 1.1 million cancer-related deaths expected globally by 2030.^{3,4} Conventional approaches to colorectal cancer treatment typically involve a combination of surgical procedures, chemotherapy, and radiotherapy. Nonetheless, the adverse effects of these treatments stem from their lack of specificity, leading to cytotoxicity against all rapidly dividing cells, including healthy ones, resulting in numerous side effects. More than half of patients had an advanced diagnosis, and it has been found that the 5-year survival rate for those with colorectal cancer is 14%.^{5–7} Moreover, despite undergoing multiple treatments, many patients face the distressing challenge of relapse. Therefore, the development of alternative and efficacious therapies for colorectal cancer becomes imperative. Immunotherapy emerges as a promising contender in cancer care, harnessing the body's immune system to combat malignant

cells.^{8–10} Unlike traditional chemotherapy and radiotherapy, immunotherapy circumvents the issue of nonspecificity, sparing normal cells devoid of cancer antigens from harm. While some cases have witnessed remarkable outcomes with cancer immunotherapy, its effectiveness varies depending on the individual's immune system status. Patients who respond favorably to immunotherapy generally experience improved prognoses and enhanced quality of life. Thus, it is essential to create alternative treatments with low toxicity in order to reduce side effects and improve clinical therapy.

Traditional herbal medicine has gained widespread acceptance as an essential alternative and supplementary medicine that benefits cancer patients.¹¹ Many studies have found that traditional medicinal plants, when taken as adjuvant treatment with radiotherapy, immunotherapy or chemotherapy, can

Received: February 23, 2024

Revised: April 15, 2024

Accepted: April 18, 2024

Published: May 1, 2024



increase quality of life, lengthen survival time, lessen side effects, and boost therapeutic effects.^{12–14} Owing to its efficiency and lack of negative side effects, the vital medicinal plant *Curcuma aromatica* Salisb (Cur) has been extensively utilized in traditional medicine.^{15–17} Several studies have showed the beneficial anticancer benefits of Cur. According to studies, Cur significantly reduces the risk of developing esophageal cancer via halting the reduction of manganese superoxide dismutase in the esophageal epithelium.¹⁸ Moreover, extracts of the Cur significantly reduce the number of hepatocellular carcinoma cells and promote tumor cell death.¹⁹ In addition, oral administration of Cur suppresses colorectal cancer progression in mice with CT26 tumors via regulating the gut microbiota.²⁰ Cur also contains numerous components, targets, and pathways to combat tumors, just like other traditional herbal medicine formulations. However, the majority of its bioactive components and pharmacological molecular mechanisms against colorectal cancer remain poorly understood. In this paper, we explored and validated the molecular processes and pathways by which Cur inhibited colorectal cancer through its primary active components using network pharmacology and biological experiments. This study will help lay the theoretical groundwork for the clinical use of Cur in colorectal cancer therapy.

METHODS AND MATERIALS

Active Ingredients of Cur. Cur compounds were obtained from the TCMSP database (<https://tcmsp-as.com/>), and the active components of Cur were screened with drug-like (DL) ≥ 0.18 and oral bioavailability $\geq 30\%$. The bioactive ingredients that do not meet the above conditions but have obvious pharmacodynamic effects were supplemented by a literature search. The molecular weight of Cur in this study is 368.38. Cur rhizome extracts were provided by the School of Pharmacy, Guangxi University of Traditional Chinese Medicine, for further *in vivo* and *in vitro* experiments.

Prediction of Target of Active Ingredients. These active ingredients are imported into TargetNet (<http://targetnetdss.scbdd.com/home/index/>), SwissTargetPrediction (<http://www.swisstargetprediction.ch/>), and TCMSP for target prediction. In order to improve the confidence of the result, the SwissTargetPrediction Web site selected the first 15 items, and the TargetNet Web site selected the results with Prob ≥ 0.9 . The predicted targets were entered in the UniProtKB database (<https://www.uniprot.org/>) and given standard gene names.

Target Collection Related to Colorectal Cancer. Colorectal cancer-related targets were searched from the GeneCards database (<https://www.genyuecayurds.org/>), the PharmGKB database (<https://www.pharyujmgb.org/>), the DisGeNET database (<https://www.disgenet.org/>), and the CTD database (<http://ctdbase.cccorg/>). The colorectal cancer-related targets obtained from these databases were summarized and deduplicated. Cur's potential targets in colorectal cancer therapy were chosen from the intersection of active ingredient targets and colorectal cancer-related targets.

FDA-Approved Anticancer Drugs and Targets. The DrugBank database (<https://go.drugbank.com/>) was used to obtain FDA-approved drugs and targets for colorectal cancer therapy, and the data were then imported into the Cytoscape software to build a drug-target network.

PPI Network Construction. A protein–protein interaction (PPI) network was created through the STRING database. The species was set to “Homo sapiens” and the confidence level to “medium confidence (0.400),” and the potential targets of Cur were entered for colorectal cancer therapy in the “many proteins” column. Finally, the collected data were loaded into the Cytoscape software for visualization and analysis of key targets.

Functional Enrichment Analysis. Using RStudio, the “clusterProfiler” R package was selected, a p-value of 0.01 was specified, and the ggplot2 package was used to plot the significant enrichment data for the KEGG and GO pathways.

Molecular Docking. In molecular docking tests, the interaction between the important targets and their corresponding ligands was verified using the docking tool “AutoDock Vina”. The protein crystal structures were obtained from the RCSB PDB database, and the compounds were downloaded from the TCMSP database. The protein crystal and compound structure were processed using AutoDock Tools, which also removed the protein structure's original ligand, charged the structure, added charges, and converted it to “PDBQT” format. The outcomes of the docking and mapping analysis modes were then retrieved using Vina docking.

Cell Culture. Human normal colonic cells NCM-460 and colorectal cancer cells HCT116 and DLD-1 were purchased from the American type culture collection (American). The 1640 medium, which contains 10% fetal bovine serum (FBS), 1% penicillin, and 1% streptomycin, was used to cultivate HCT116 and DLD-1 cells. The incubator (Thermo Forma 3111, Thermo Fisher Scientific, Inc., Waltham, MA, USA) is designed to operate at 37 °C with 5% CO₂.

Cell Activity Detection. Once the cell density was increased to 4×10^5 /well in 6-well plates, HCT116 and normal colonic cells (NCM-460) at the logarithmic growth stage were plated on 96-well plates. After cell adhesion, the cells were then cultured with various concentrations of Cur extract (provided by the School of Pharmacy, Guangxi University of Traditional Chinese Medicine) for 24 h, and counting kit-8 (CCK8) reagent (Beyotime, China) was added. After that, the OD value at 450 nm wavelength was detected by an enzyme labeling instrument according to CCK-8 instructions.

Scratch Test. Cells at the logarithmic growth stage were inoculated in 6-well plates until the cells grew to 80–90%. A line was marked in the middle with a 200 μ L gun head and rinsed with phosphate-buffered saline (PBS) for postdosing treatment. 24 h later, they were observed again and photographed.

Cell Invasion and Migration Experiment. The ability of cells to migrate and invade was examined using the Transwell assay. Migration experiments: A serum-free medium was used to collect logarithmic growth cells and adjust the cell density of digestive cells to 2×10^6 /mL. The lower chamber received 700 μ L of medium containing 20% FBS, whereas the upper chamber received 200 μ L of cell suspension. After 48 h of incubator culture, the upper compartment cells were fixed after being cleaned with PBS and cotton swabs. 0.1% of crystal violet was used to stain the cells for observation and statistics. Invasion experiments: Matrigel glue was mixed with serum-free medium and spread in a cold chamber. The chamber was placed in an orifice plate and solidified into a gel overnight in a

Table 1. Active Ingredients of *Curcuma aromatica* Salisb

MOL_ID	molecule_name	ob	dl
MOL000358	beta-sitosterol	36.91390583	0.75123
MOL000359	sitosterol	36.91390583	0.7512
MOL000908	beta-elemene	25.63362343	0.060519
MOL004237	δ -elemene	25.99022265	0.060207
MOL004241	curcolactone	51.50981617	0.19615
MOL004244	(4aR,5R,8R,8aR)-5,8-dihydroxy-3,5,8a-trimethyl-6,7,8,9-tetrahydro-4aH-benzo[f]benzofuran-4-one	59.51959947	0.19518
MOL004253	curcumenolactone C	39.70086781	0.18868
MOL004260	(E)-1,7-diphenyl-3-hydroxy-1-hepten-5-one	64.66064017	0.18319
MOL004262	deta-elemene	23.56025572	0.060299
MOL004263	(E)-5-hydroxy-7-(4-hydroxyphenyl)-1-phenyl-1-heptene	46.89753325	0.19423
MOL004291	oxycurcumenol	67.06408444	0.18343
MOL004305	zedoalactone A	111.4268876	0.18825
MOL004306	zedoalactone B	103.5929022	0.21754
MOL004309	zedoalactone E	85.16477434	0.19062
MOL004311	zedoanolide A	87.96501883	0.29704
MOL004313	zedoanolide B	135.5563917	0.21409
MOL004316	1,7-diphenyl-3-acetoxy-6(E)-hepten	48.47077905	0.22242
MOL004328	naringenin	59.29389773	0.21128

constant-temperature incubator. The subsequent experimental operation is consistent with the transfer experiment.

Plate Clone Formation Assay. After cell density was adjusted to 2×10^3 /well in 6-well plates, HCT116 and DLD-1 cells were inoculated into 96-well plates at logarithmic growth stages. Then, different concentrations of Cur extract were added and incubated for 7 days. Crystal violet 0.1% was used to dye the cells after they were fixed with 4% paraformaldehyde. The number of stained colonies was counted to detect clonal formation.

Flow Cytometry Experiment. HCT116 and DLD-1 cells were inoculated into 6-well plates (cell density was 1×10^5). After the cells adhered to the wall, the original medium was discarded, and different concentrations of Cur extract were added and incubated for 48 h. After the cells were collected, they were washed with PBS and resuspended in $1 \times$ annexin V binding solution (cell density adjusted to 1×10^6 /well). Cell suspension ($100 \mu\text{L}$) was taken into the flow tube, and $5 \mu\text{L}$ of PI and Annexin V-FITC were added and cultured for 15 min at room temperature. After adding $500 \mu\text{L}$ of PBS, the cell apoptosis rate was detected by a flow cytometer (Multiskan Go 1510, Beckman, USA).

Western Blot. Cells and tissues were lysed using radio immunoprecipitation assay (RIPA) lysate, which contains a protease inhibitor, in order to extract total protein. The proteins from the colorectal cancer cells and tissue were extracted by a protein extraction kit. The protein sample was boiled after the BCA kit had been used to quantify the protein. After SDS-PAGE, the samples were transferred to a PVDF membrane, sealed with 5% skim milk, and then exposed to the primary antibody at $4 \text{ }^\circ\text{C}$ for an overnight incubation. The secondary antibody was incubated at room temperature after being rinsed with TBS with Tween-20 (TBST), and the ECL chemiluminescence developer was uniformly applied for detection on the gel imaging device. Primary antibodies include AKT1 (dilution ratio of 1:1000, ab81283, Abcam), pAKT1 (dilution ratio of 1:1000, ab183556, Abcam), PTGS2 (dilution ratio of 1:200, ab255420, Abcam), p53 (dilution ratio of 1:200, ab32049, Abcam), estrogen receptor 1 (ESR1) (dilution ratio of 1:200, ab108398, Abcam), Bcl-2 (dilution ratio of 1:1000, ab32124, Abcam), Bax (dilution ratio of

1:1000, ab32503, Abcam), and β -actin (dilution ratio of 1:2000, sc-8432, Santa Cruz Biotechnology). Secondary antibodies were HRP-labeled goat antimouse IgG (H + L) (dilution ratio of 1:1000, ab150116, Abcam) and HRP-labeled goat antirabbit IgG (H + L) (dilution ratio of 1:1000, ab6721, Abcam). The protein bands were visualized by the Tanon 5500 Imaging System (Tanon Technology Co. Ltd., Shanghai, China).

REAL-TIME QUANTITATIVE PCR

TRIzol extraction kits (Invitrogen, America) were used to extract RNA from cells. A high-capacity cDNA reverse

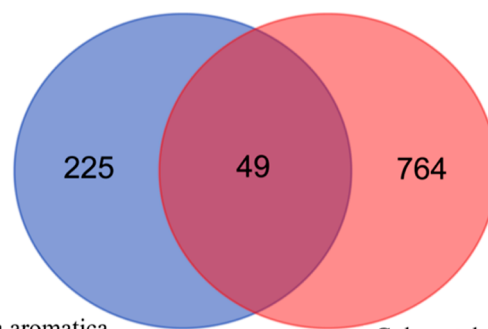


Figure 1. Intersection of active component targets of Cur and colorectal cancer-related targets.

transcription kit (Takara, Kyoto, Japan) was used to create the first strand of complementary DNA. qRT-PCR was then done on an ABI7900HT fast real-time PCR system (Applied Biosystems, Foster City, CA, USA) for 40 cycles ($60 \text{ }^\circ\text{C}$ for 1 min, $90 \text{ }^\circ\text{C}$ for 15 s, and $95 \text{ }^\circ\text{C}$ for 3 min). The primer sequences for real-time PCR were as follows: AKT1-forward sequence, 5'-GACGGGCACATTAAGATCAC-3'; reverse sequence, 5'-TGAGGATGAGCTCAAAAAGC-3'. PTGS2-forward sequence, 5'-GCTACAAAAGCTGGGAA-3'; reverse sequence, 5'-CTGATGCGTGAAGTGCTG-3'. TPS3-forward sequence, 5'-TAACAGTTCCTGCATGGGCGGC-3'; reverse sequence, 5'-AGGACAGGCACAAAACGCACC-3'. ESR1-forward sequence, 5'-TTACTGACCAACCTGGCAGA-3';

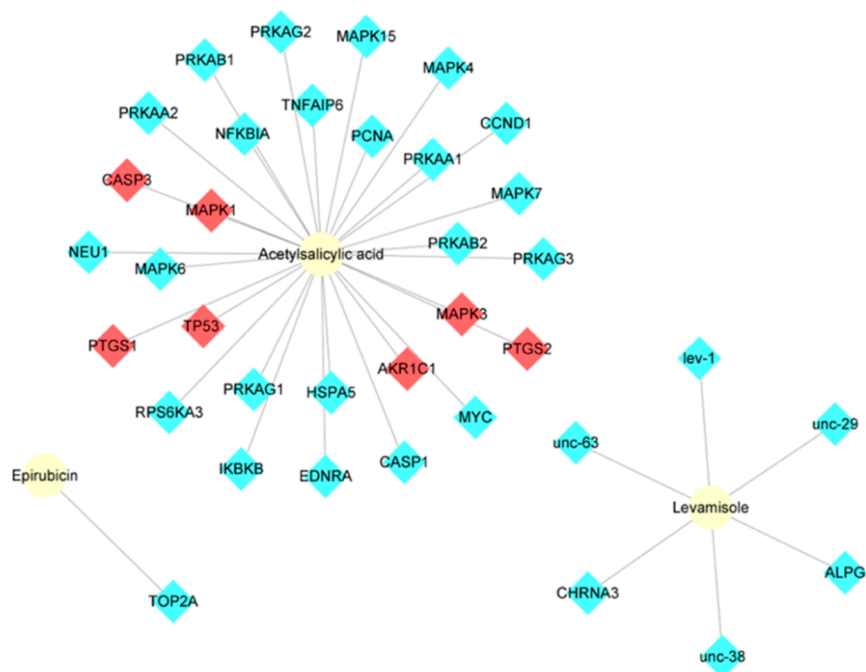


Figure 2. Intersection of active ingredient targets in Cur and drug targets approved by the FDA.

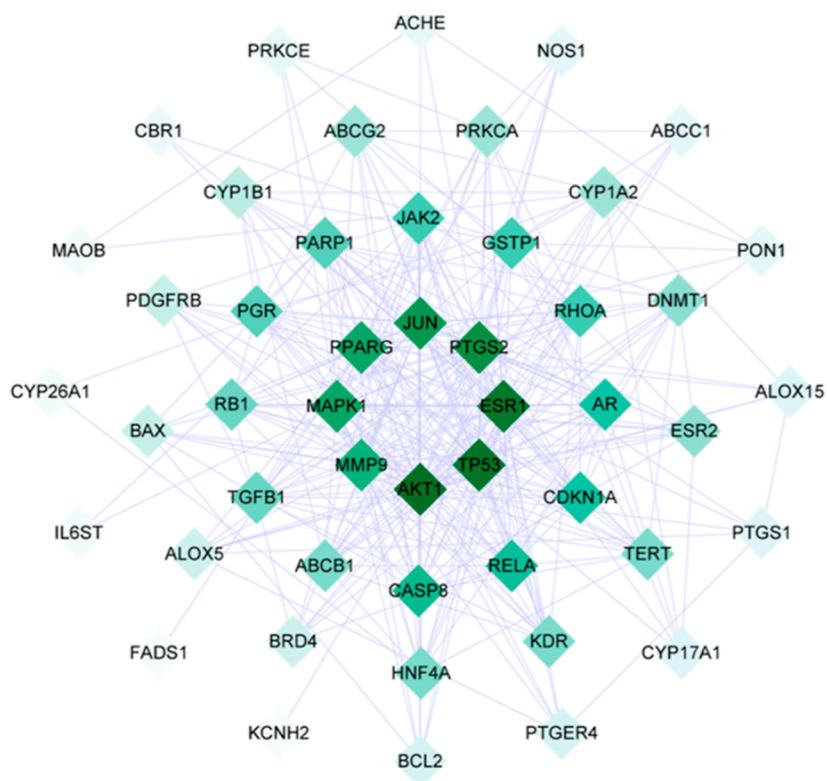


Figure 3. Protein–protein interaction (PPI) network.

reverse sequence, 5'-ATCATGGAGGGTCAAATCCA-3'. Bcl-2-forward sequence, 5'-GTTTCGGTGGGGTCATGTGTGTGGAGAGCG-3'; reverse sequence, 5'-TAGCTGATTCGACGTTTGCCTGA-3'. Bax-forward sequence, 5'-CTGACATGTTTTCTGACGGC-3'; reverse sequence, 5'-TCAGCCCATCTTCTTCCAGA-3'. β -Actin-forward sequence, 5'-GACCTCTATGCCAACACAGT-3'; reverse sequence, 5'-AGTACTTGCGCTCAGGAGGA-3'. For mRNA,

the internal control of qRT-PCR was β -actin. Melting curve analysis was used to assess the specificity of all PCR products. The $2^{-\Delta\Delta C_t}$ method was used to determine relative gene expression.

Animal Experiments. Ten female BALB/c-nu nude mice at 5 weeks of age and weighing 18–22 g were purchased from Hunan SJA Laboratory Animal Co., Ltd. They were housed in a barrier environment at the SPF level and allowed to

Table 2. Screening of Key Targets in the PPI Network

top 10 in network ppi.txt ranked by the degree method			top 10 in network ppi.txt ranked by the betweenness method			top 10 in network ppi.txt ranked by the closeness method		
rank	name	score	rank	name	score	rank	name	score
1	AKT1	35	1	AKT1	281.68	1	AKT1	41.33
2	TP53	34	2	ESR1	244.17	2	TP53	40.67
3	ESR1	33	3	PPARG	215.98	3	ESR1	40.33
4	PTGS2	28	4	CYP1A2	187.94	4	PTGS2	37.67
5	JUN	27	5	TP53	180.84	5	JUN	37.17
6	PPARG	25	6	PTGS2	152.48	6	MAPK1	36.17
7	MAPK1	25	7	MAPK1	126.28	7	PPARG	35.83
8	MMP9	23	8	HNF4A	91.24	8	MMP9	35.17
9	CASP8	21	9	GSTP1	62.08	9	CASP8	34.00
10	RELA	20	10	JUN	56.00	10	RELA	33.50

acclimatize for 1 week. The mice were then randomly divided into two groups: a model group ($n = 5$) and a Cur group ($n = 5$) for the experiment. The HCT116 colorectal cancer cell line was cultured, and logarithmic growth phase cells were collected. The cells were prepared as a single-cell suspension using PBS and adjusted to a concentration of 1×10^7 cells/mL. The cells were then subcutaneously injected into the armpits of BALB/c-nu mice at a dose of 0.2 mL per mouse. Beginning on the second day after injection, the mice were orally administered Cur (100 mg/kg) once a day for 27 days. Of note, we systematically administered the extract to mice at 100 mg/kg, which is reasonable and consistent with previous literature reports as safe and effective.^{18,21,22} During the experiment, the weight and tumor volume of the mice were measured every 3 days until the end of the study. The formula for calculating tumor volume was $V = 0.5 LW^2$, where L is the longest diameter of the tumor (mm) and W is the shortest diameter of the tumor (mm). At the end of the experiment, the mice were euthanized with pentobarbital sodium anesthesia, and the subcutaneous tumors were removed and weighed. The transplanted tumors were observed by an inverted microscope (BX51, Olympus Corporation, Japan). All procedures were carried out in accordance with the University of South China Animal Care Guidelines and the Institutional Animal Ethics Committee for the Use of Experimental Animals (approval number: SYXK (Hunan) 2020-0002).

HE Assays. The transplanted subcutaneous tumors were fixed with paraformaldehyde, embedded in paraffin, and sectioned. After deparaffinization and dehydration, the sections were stained with hematoxylin for 5 min, washed, differentiated with hydrochloric acid alcohol, counterstained with eosin, and then dehydrated and mounted for observation.

Immunohistochemistry. For paraffin sections, deparaffinization and dehydration were first carried out, followed by antigen retrieval to eliminate the influence of endogenous peroxidase. The sections were then blocked, and the corresponding primary antibody was incubated overnight at 4 °C. After incubation with the secondary antibody, DAB staining was performed. Finally, the sections were counterstained with hematoxylin, mounted with neutral resin, and observed.

Data Analysis. The mean and standard deviation of the data from three distinct experiments are shown (SD). A one-way ANOVA was used to assess how different the groups were from one another, and the Student's *t*-test was used to compare the means of the two groups. GraphPad software (version 8.0.1) and SPSS 24.0 were used to conduct all statistical

analyses. Statistics were considered significant when the *P* value was <0.05 .

RESULTS

Results of Query on Active Ingredients of Cur. The results of the literature supplement and TCMSP database

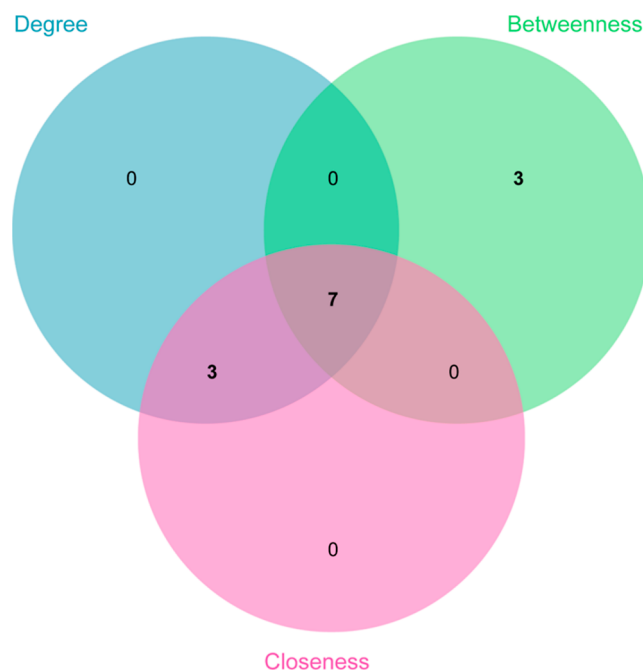


Figure 4. Screening of key targets.

searches yielded a total of 18 active substances, as shown in Table 1.

Prediction Results of Target of Active Ingredients. The obtained active ingredients were imported into the Web sites TCMSP, SwissTargetPrediction, and TargetNet for target prediction. After the gene names were standardized through the UniProtKB database, a total of 274 active ingredient targets were obtained.

Colorectal Cancer-Related Targets. The PharmGKB, CTD, DisGeNET, and GeneCards databases were respectively searched to obtain relevant targets for colorectal cancer. To improve the reliability of results, only targets with “marker/mechanism (M)” or “therapeutic” markers were selected in the CTD database, and results with a relevance score ≥ 20 were selected in the GeneCards database. By summing and

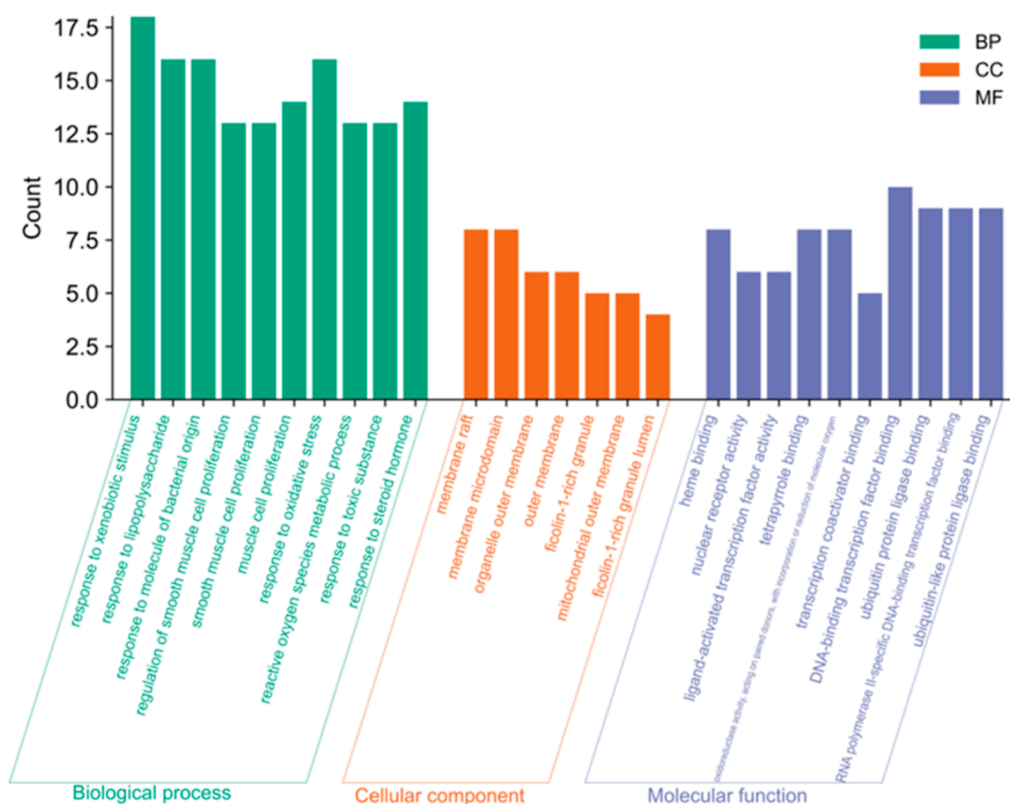


Figure 5. GO enrichment analysis.

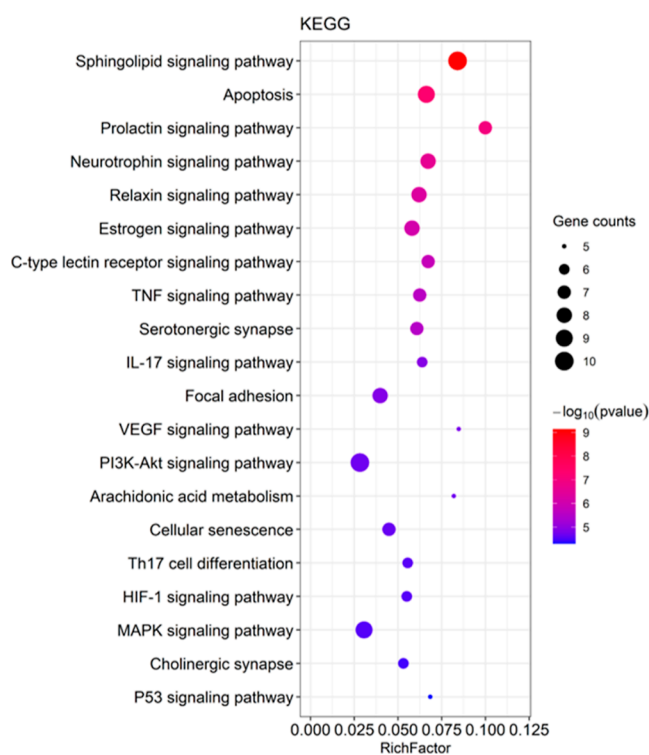


Figure 6. Enrichment analysis of KEGG biological pathways.

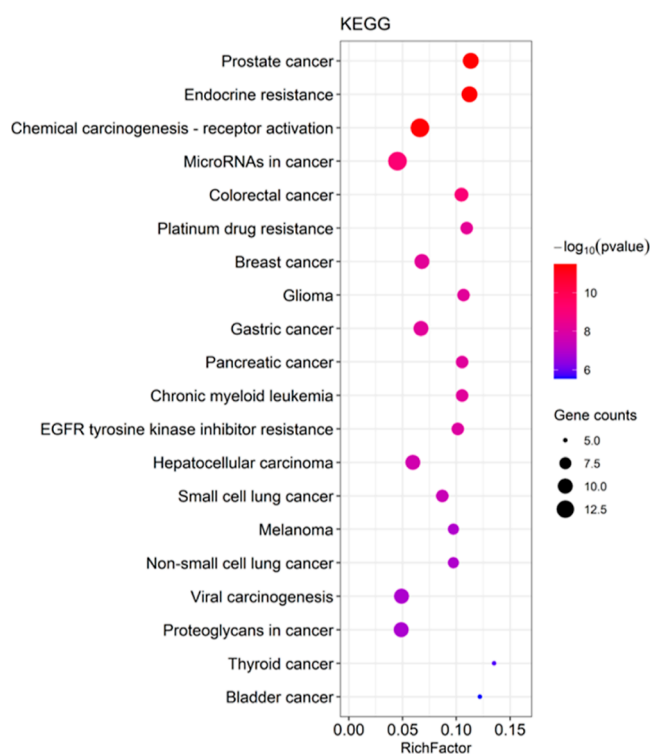


Figure 7. Enrichment analysis of KEGG disease pathways.

deweighting the targets acquired from each database, a total of 813 colorectal cancer-related targets were found. As shown in Figure 1, the intersection of the active ingredient targets of Cur and targets associated with colorectal cancer resulted in the

selection of 49 targets as possible targets for Cur in colorectal cancer therapy.

FDA-Approved Anticolorectal Cancer Drugs and Targets. A search of the DrugBank database yielded 3 FDA-approved small-molecule medications for colorectal cancer,

Table 3. Docking Results of Key Target Molecules

	AKT1	ESR1	PTGS2	TP53
MOL000358	-3.8	-6.4	-4.7	-6.3
MOL000359	-0.8	-5.5	-3.1	-5.5
MOL000908	-6.5	-7.3	-7.1	-4.7
MOL004237	-5.6	-7.2	-7.1	-4.3
MOL004241	-5.2	-7.9	-5.5	-5.3
MOL004244	-7.4	-7.6	-6.5	-5.7
MOL004253	-6.6	-7.8	-9	-5.3
MOL004260	-7.8	-7.1	-8.4	-6.7
MOL004262	-4.6	-7.5	-6.7	-4.5
MOL004263	-8	-7.5	-8.4	-6
MOL004291	-5.9	-7.7	-5.8	-5.3
MOL004305	-7	-8	-6.3	-6
MOL004306	-4	-6.9	-6.6	-5.5
MOL004309	-4.6	-7.3	-8	-5.6
MOL004311	-4.9	-8.2	-4	-5.7
MOL004313	-4	-8.2	-4.7	-5.4
MOL004316	-7.8	-8.5	-8.6	-6.4

which correspond to a total of 36 validated targets, 7 of which were shared targets between Cur and FDA-approved drugs. To create the drug-target network, FDA-approved therapeutic drugs and their matching targets are entered into the Cytoscape program. As shown in Figure 2, diamonds represent targets, circles represent drugs, and red nodes are common targets of Cur and FDA-approved drugs. The results suggest that Cur has the same or similar effects as these drugs with overlapping targets. It is important to note that the presence of a common target does not necessarily imply the same mechanism of action. In our analysis, we aimed to identify common targets between our extracts and drugs marketed on the market to gain insight into potential similarities in their pharmacological effects. However, it needs to be acknowledged that the degree of overlap of targets for different drugs may vary, and our results do show variations in the number of common targets. In addition, we recognize that our study provides a snapshot of potential target interactions based on data available in DrugBank's database. Further experimental validation and in-depth analysis are needed to confirm the

Table 4. Content of 13 Active Components in Cur Root Extract and the Total Dry Extract Yield

name	alcohol extract
gallic acid/(mg·g ⁻¹)	17.99 ± 0.10c
geniposide/(mg·g ⁻¹)	98.33 ± 0.21c
paeoniflorin/(mg·g ⁻¹)	188.60 ± 0.20c
chebulinic acid/(mg·g ⁻¹)	160.60 ± 0.69c
coptisine/(mg·g ⁻¹)	26.70 ± 0.10c
baicalin/(mg·g ⁻¹)	118.27 ± 0.3c
berberine hydrochloride/(mg·g ⁻¹)	111.47 ± 0.06c
wogonoside/(mg·g ⁻¹)	22.50 ± 0.52c
baicalein/(mg·g ⁻¹)	31.80 ± 0.03c
wogonin/(mg·g ⁻¹)	11.80 ± 0.01c
curcumin/(mg·g ⁻¹)	1.50 ± 0.01c
emodin/(mg·g ⁻¹)	41.80 ± 0.02c
chrysophanol/(mg·g ⁻¹)	0.05 ± 0.003c
total proportion/%	83.141 ± 0.003c
otal dry extract yield/%	31.39 ± 0.05c

functional relevance of these target interactions and their impact on anticancer activity.

Core Targets Were Obtained by Constructing Protein–Protein Interaction Networks. A visualization tool called Cytoscape was used to import the PPI network of possible therapeutic targets. There are 325 interactions among 49 targets (Figure 3). The color of the nodes in the diagram changes from light to dark, indicating that the node's degree value increases from small to large. The key targets (Top10) were determined according to degree, betweenness, and closeness using the plugin cytoHubba to calculate the topological properties of the network's nodes. The intersection of targets obtained by three methods was taken as the key target of the PPI network. As shown in Table 2 and Figure 4, AKT serine/threonine kinase 1 (AKT1), tumor protein p53 (TP53), ESR1, prostaglandin-endoperoxide synthase 2 (PTGS2), Jun, peroxisome proliferator-activated receptor gamma, and mitogen-activated protein kinase 1 may be the pivotal targets of Cur in the treatment of colorectal cancer.

Functional Enrichment Analysis. Enrichment analysis of potential therapeutic targets using RStudio yielded 1358 GO

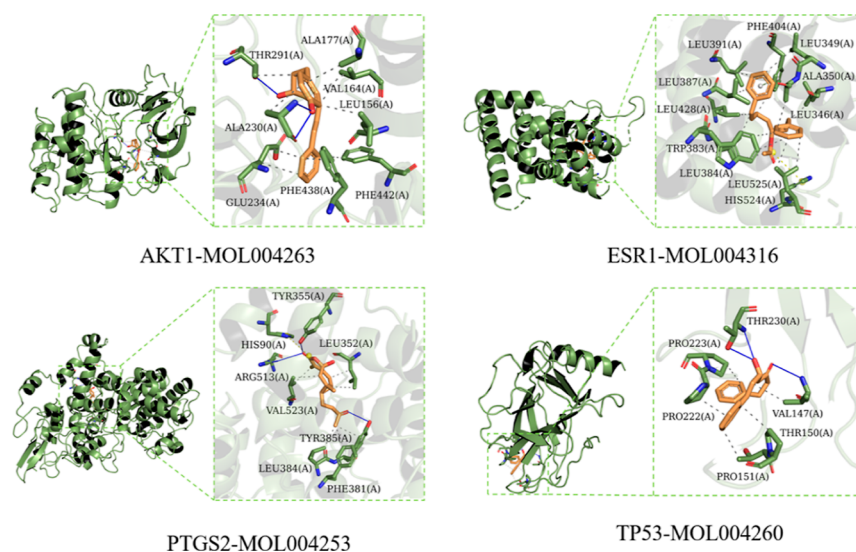


Figure 8. Schematic diagram of molecular docking.

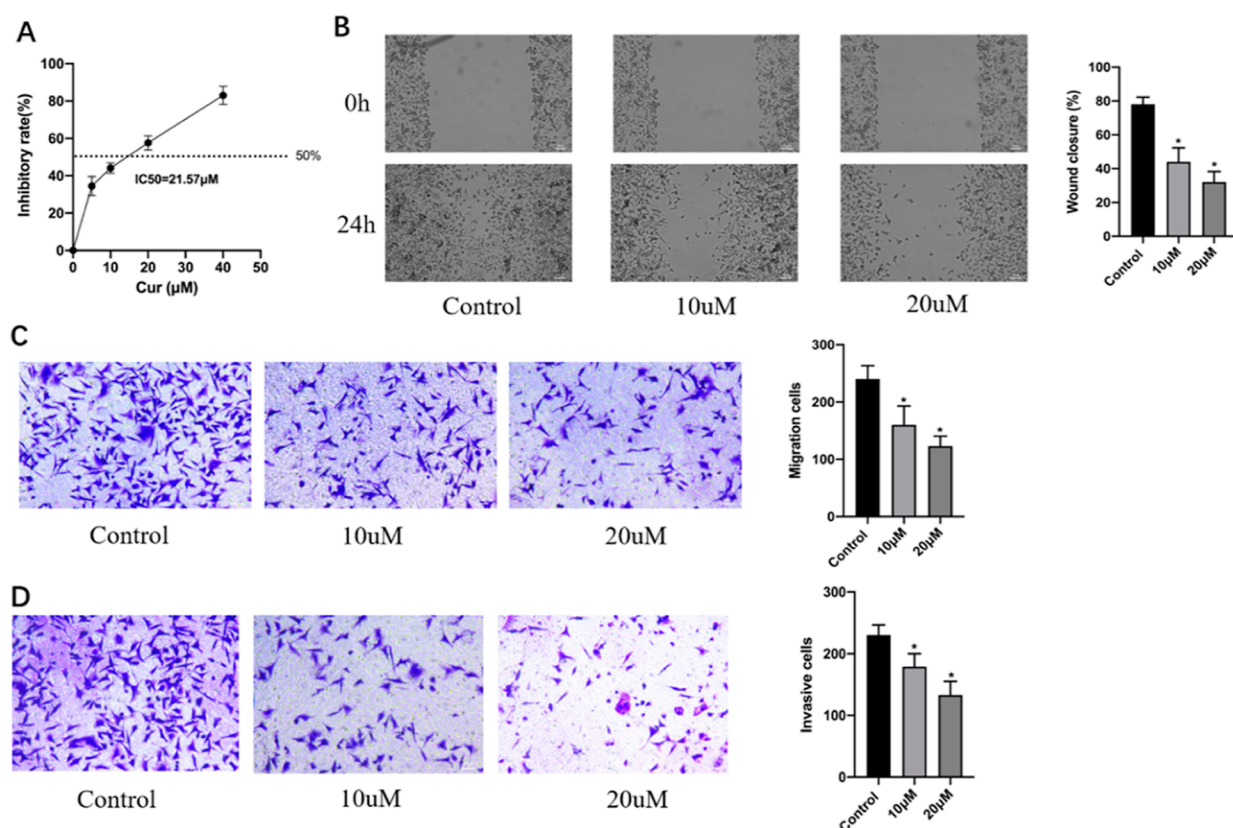


Figure 9. Effects of Cur on the proliferation, invasion, and migration of human colorectal cancer cells. (A) Cell activity was detected by the CCK-8 assay. (B) Cell proliferation was determined by the scratch assay. (C) Cell migration was measured by the transwell experiment. (D) Cell invasion was detected by the transwell experiment. * $p < 0.05$ vs control.

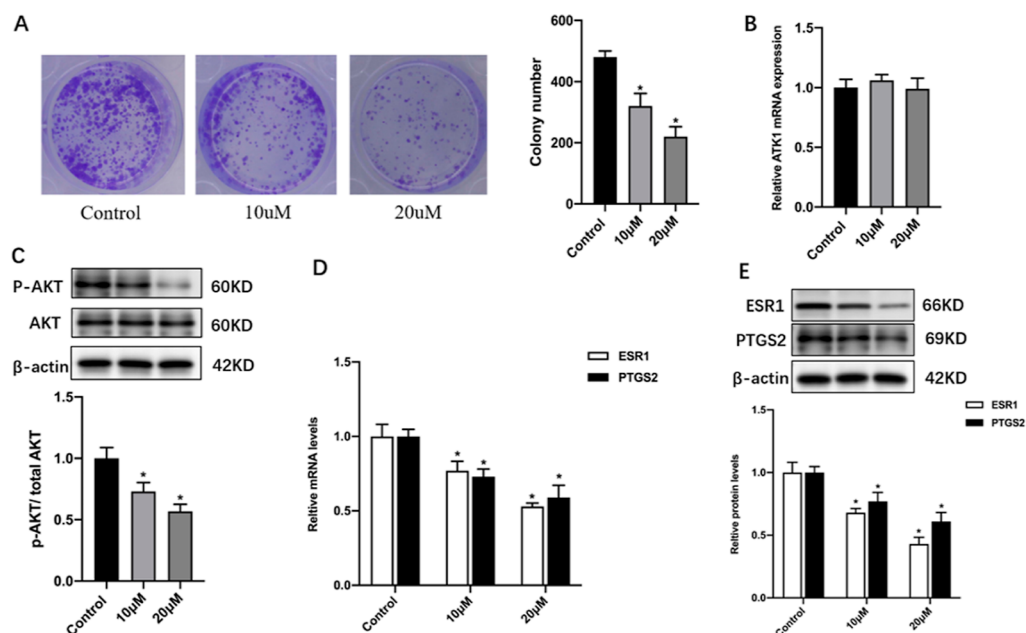


Figure 10. Effects of Cur on the expression of AKT1, ESR1, and PTGS2. (A) Cell colony formation. (B) AKT mRNA, (C) AKT protein, and p-AKT phosphorylation expression were detected by WB and qRT-PCR. (D) ESR1 and PTGS2 mRNA and (E) protein expressions were detected by qRT-PCR and WB, respectively. * $p < 0.05$ vs control.

items, 760 of which were biological process (BP), 7 pieces of cellular component, and 50 pieces of molecular function. These items cover biological roles such as response to xenobiotic stimuli, response to lipopolysaccharide, response

to bacterial molecules, and regulation of smooth muscle cell proliferation (Figure 5). These findings suggest that Cur protects against colorectal cancer by the regulation of cell proliferation and migration.

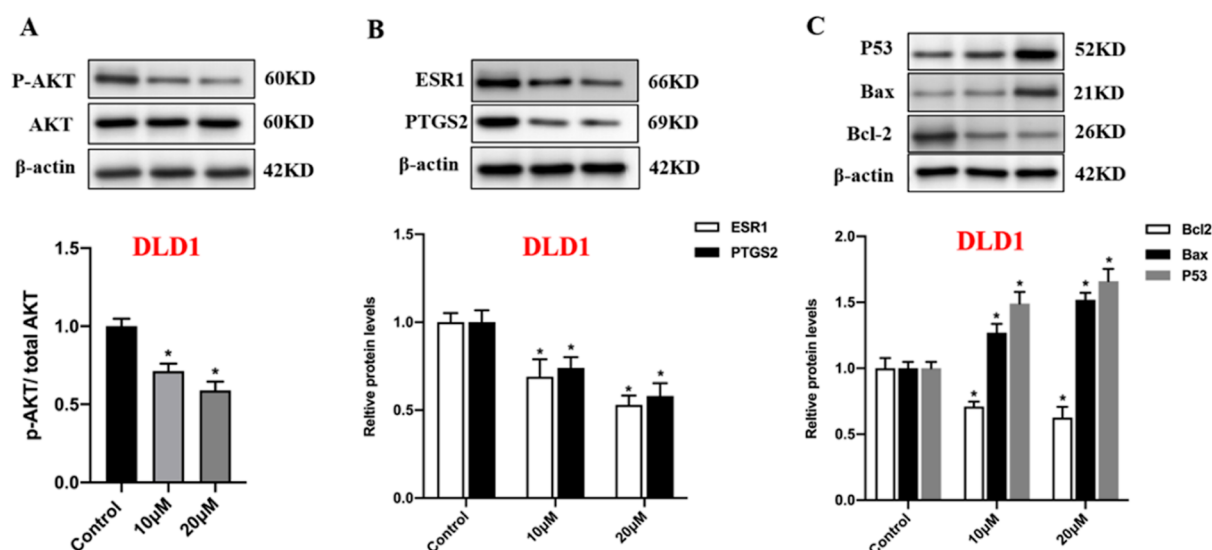


Figure 11. Effects of curcuma aromatica on proliferation- and apoptosis-related protein expressions in DLD-1 colon cancer cell lines. (A) p-AKT phosphorylation and AKT protein expressions were detected by WB. (B) PTGS2 and ESR1 protein expressions were detected by WB. (C) Apoptosis-related protein expressions were detected by WB. * $p < 0.05$ vs control.

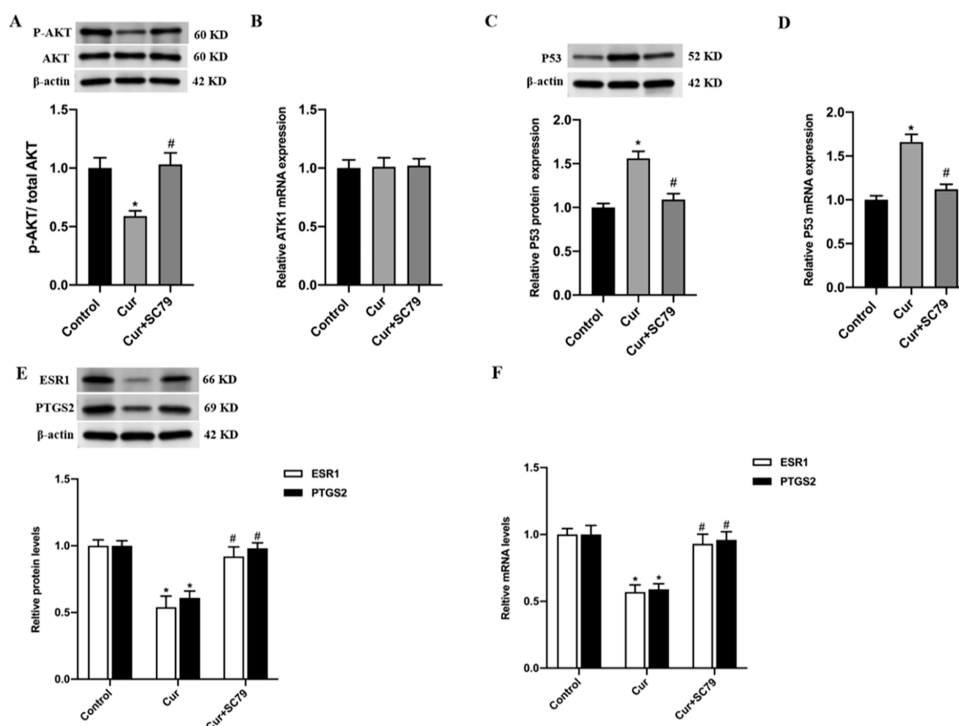


Figure 12. Effects of AKT1 agonist on Cur-regulated expression of TP53, ESR1, and PTGS2. (A) p-AKT phosphorylation, AKT protein, and (B) AKT mRNA expression were detected by WB and qRT-PCR. TP53 (C) protein and (D) mRNA expressions were detected by WB and qRT-PCR, respectively. PTGS2 and ESR1 (E) protein and (F) mRNA expressions were detected by qRT-PCR and WB, respectively. * $p < 0.05$ vs control.

The study of the KEGG enrichment of possible therapeutic targets was carried out using RStudio. The pathway of the fundamental BP was established using the KEGG pathway enrichment data. Five sections of the KEGG database yielded a total of 77 significantly enriched pathways. The TNF, IL-17, VEGF, and PI3K-Akt signaling pathways may be the key pathways of Cur in colorectal cancer therapy (Figure 6). As shown in Figure 7, Cur, according to KEGG enrichment results, primarily intervenes in prostate cancer, endocrine resistance, chemical carcinogenesis-receptor activation, and colorectal cancer.

Molecular Docking Results. According to the above-mentioned results, key proteins PTGS2, ESR1, TP53, and AKT1 were chosen for molecular docking experiments with Cur to confirm their interactions. As shown in Table 3, molecular docking results had binding energies that were significantly lower than -5 kcal/mol, suggesting that the target proteins and ingredients have a high affinity for binding. As shown in Figure 8, the docking mode was investigated in conjunction with the outcomes of strong docking activities. This result showed that the active components of Cur entered the active site and connected with essential amino acid

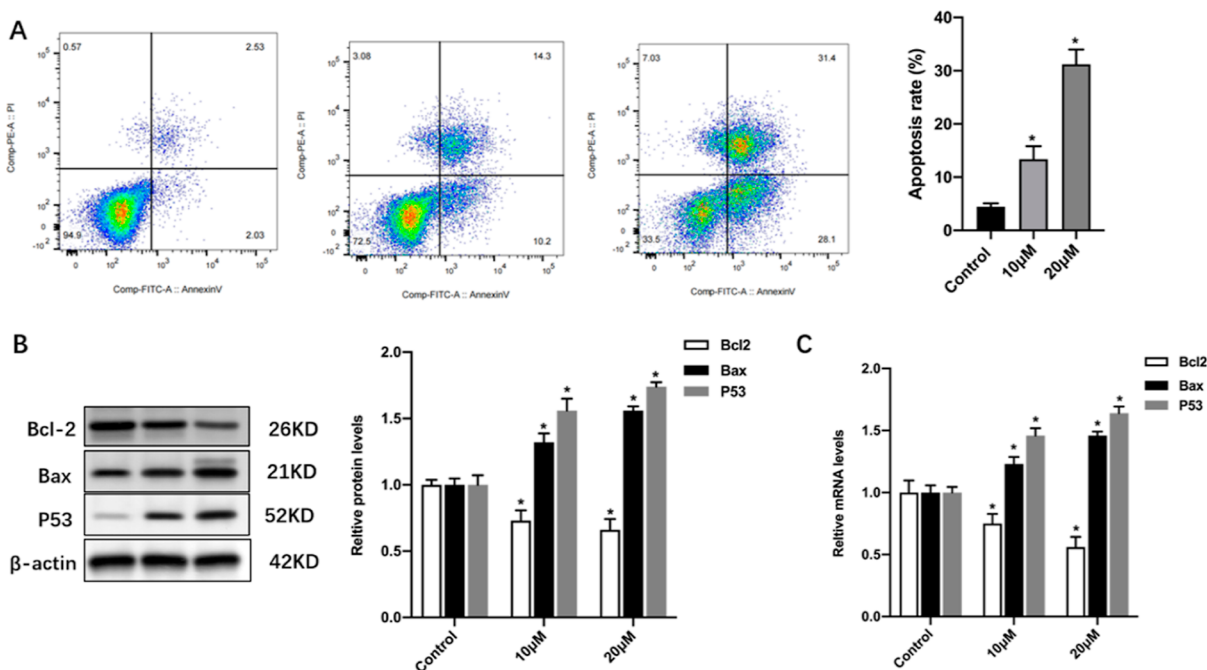


Figure 13. Effects of Cur on the apoptosis of human colorectal cancer cells. (A) Cell apoptosis was detected by the flow cytometry experiment. Apoptosis-related (B) protein and (C) mRNA expressions were detected by WB and qRT-PCR, respectively. * $p < 0.05$ vs control.

residues via polar or nonpolar connections to stabilize the ligand–receptor interaction. These results further demonstrate that PTGS2, ESR1, TP53, and AKT1 screened by the network pharmacology of Cur play a key role in the treatment of colorectal cancer.

Cur Inhibits the Proliferation, Invasion, and Migration of Human Colorectal Cancer Cells. To explore the in vitro effect of Cur on colorectal cancer, HCT116 and DLD-1 cells were treated with different concentrations of Cur extract. The contents of 13 active components in Cur extract and the yield of total dry extract are shown in Table 4. The CCK-8 assay showed that the extract markedly suppressed the proliferative activity of HCT116 cells, and the IC₅₀ was 21.57 μM (Figure 9A). The cytotoxicity of Cur to NCM-460 human normal colonic epithelial cells was detected (supplementary Figure S1), which showed that treatment with Cur at 2.5 μM, 5 μM, 10 μM, and 20 μg/mL did not significantly attenuate the viability of NCM-460 cells. Therefore, 10 and 20 μM Cur root extracts were selected for subsequent experiments. Furthermore, cell scratch and transwell experiments also showed that Cur inhibited the proliferation, invasion, and migration of HCT116 cells (Figure 9B–D). Moreover, the cloning experiment showed that, compared with the untreated group, Cur significantly inhibited cell colony formation (Figure 10A). Network pharmacology and molecular docking experiments showed that the active components of Cur had a good affinity with AKT1, TP53, ESR1, and PTGS2. Also, numerous studies have shown that AKT1, ESR1, and PTGS2 are involved in the proliferation and migration of colorectal cancer cells.^{23–26} Thus, WB assays were carried out to further verify the effect of Cur on the expression of these core targets. The results showed that Cur significantly inhibited AKT phosphorylation and decreased ESR1 and PTGS2 levels (Figures 10B–E and 11A,B). It has been reported that the activation of AKT signaling promotes the expression of ESR1, driving liver cancer progression.²⁷ Downstream of Akt, PTGS2 (also known as

COX2) has also been demonstrated to be involved in carcinogenesis.²⁸ These results suggest that AKT acts as a crucial upstream factor regulating gene expression involved in tumor progression. To explore the in-depth mechanism underlying the inhibitory effects of Cur on colorectal cancer, we treated colorectal cancer cells with 20 μM Cur followed by an AKT1 agonist. Then, pAKT1, PTGS2, and ESR1 expressions were detected. As shown in Figure 12A,B,E,F, the AKT1 agonist could revise the effects of Cur on the expression of pAKT1, PTGS2, and ESR1, suggesting that AKT1 serves as an important regulator of PTGS2 and ESR1, mediating the inhibitory effects of Cur on colorectal cancer. Collectively, these data suggest that Cur suppresses the proliferation, migration, and invasion of human colorectal cancer cells through decreasing AKT phosphorylation and downregulating ESR1 and PTGS2 expression.

Cur Facilitates the Apoptosis of Human Colorectal Cancer Cells. The results of network pharmacology and molecular docking suggest that Cur is involved in the modulation of apoptosis and colorectal cancer. The flow cytometry experiment was used to determine the effect of Cur on the apoptosis of HCT116 cells. As shown in Figure 13A, Cur significantly promoted the apoptosis of HCT116 cells. It has been reported that TP53, Bcl-2, and Bax are key proteins regulating tumor apoptosis.^{29–31} The effects of Cur on apoptosis-related proteins were further detected by WB and qRT-PCR. As shown in Figures 13B,C and 11C, Cur markedly inhibited Bcl-2 expression and increased the expression of proapoptotic proteins Bax and P53. Moreover, numerous studies have demonstrated that AKT is a key negative regulator of TP53, which plays an important role in the development of tumors.^{32,33} As shown in Figure 12C,D, our results showed that Cur could promote TP53 expression by inhibiting AKT. These data indicate that Cur facilitates the apoptosis of colorectal cancer cells, suppressing the development of colorectal cancer.

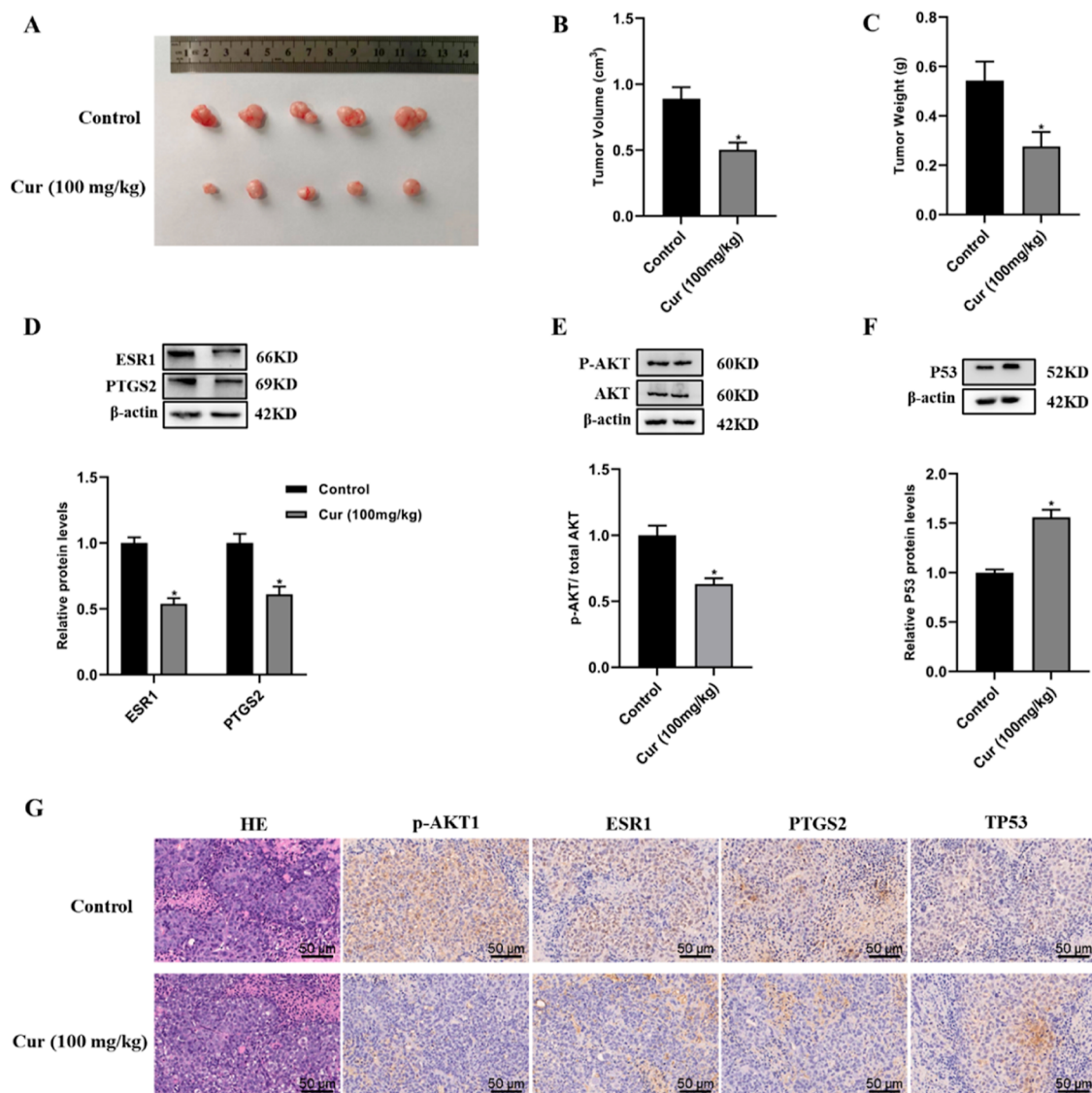


Figure 14. Effects of Cur on the growth of colorectal cancer in BALB/c-nu mice. Image of tumor (A,B) volume and (C) weight on day 27. (D) PTGS2, ESR1, (E) p-AKT phosphorylation, AKT, and (F) P53 expressions were detected by WB ($n = 5$ mice/group). (G) H&E staining of tumor tissues and immunohistochemistry staining of p-AKT1, ESR1, PTGS2, and TP53 were performed using tumor slides from different groups ($n = 5$ mice/group). * $p < 0.05$ vs control.

Cur Inhibits the Growth of Colorectal Cancer in BALB/C-Nu Mice. To investigate the anticancer effect of Cur in vivo, we chose BALB/c-nu nude mice for tumor modeling and oral administration. The results showed that, compared with the model group, Cur significantly reduced the tumor volume and weight (Figure 14A–C), suggesting that Cur has an inhibitory effect on the growth of colorectal cancer in nude mice. Also, Cur inhibited AKT phosphorylation, decreased ESR1 and PTGS2 protein levels, and increased P53 expression in colorectal cancer tissue (Figure 14D–F). Furthermore, after fixation, sectioning, and HE staining, the transplanted tumors were observed under an inverted microscope. The results showed that the cell nuclei of the tumor tissue in the model group were closely arranged and blood vessels were visible, while the tumor cells in the treated group showed shrinkage, apoptosis, and obvious necrosis. The results showed that Cur could promote the apoptosis of tumor cells and inhibit their proliferation. Based on molecular docking and cell experiments, we verified the key targets in

BALB/c-nu mice. Immunohistochemical results showed that the expression of AKT, ESR1, and PTGS2 was decreased and the expression of P53 was up-regulated after treatment with Cur (Figure 14G). These results indicated that Cur could inhibit colorectal cancer by promoting apoptosis and inhibiting the proliferation and migration of cancer cells.

DISCUSSION

The current study revealed bioactive ingredients and the molecular mechanism of Cur in the therapy of colorectal cancer by using in vitro experimental validation, molecular docking, and network pharmacology-based techniques. Our findings showed that the active ingredients of Cur displayed high affinity for AKT1, TP53, ESR1, and PTGS2, according to network pharmacology and molecular docking assays. Furthermore, our results showed that Cur significantly suppresses the growth of colorectal cancer by promoting apoptosis and inhibiting the proliferation and migration of cancer cells. Also, we found that Cur decreased the

phosphorylation of AKT, downregulated PTGS2 and ESR1 expression, and increased TP53 levels in colorectal cancer tissue and cells.

Colorectal cancer is the third most commonly diagnosed malignancy worldwide, with significant geographic heterogeneity in incidence and mortality.³⁴ The combination of network pharmacology and molecular docking technology is gradually forming a systematic paradigm, providing an unprecedented opportunity for the systematic study of traditional medicinal plants in cancer, and becoming a Frontier research field in drug discovery and development.^{35–37} It has been reported that Mufangji decoction, a famous traditional Chinese medicine formula, can treat lung cancer by multiple pathways, multiple targets, and multiple components based on network pharmacology and experimental validation.³⁸ Gao et al. also reported that aloin protects against gastric cancer by regulating the PI3K-AKT signaling pathway through integrating network pharmacology and experimental verification.³⁹ Cur is an important traditional medicinal plant that has gained popularity due to its beneficial health properties, including antitumor activity.^{40,41} In this study, our findings showed that the active ingredients of Cur have the same targets as the drug acetylsalicylic acid, suggesting that Cur exerts the same or similar antitumor pharmacological effects as acetylsalicylic acid to treat or improve colorectal cancer. Also, our results showed that these targets are involved in the modulation of cell apoptosis, migration, and proliferation. We found that Cur promotes the apoptosis of human colorectal cancer cells and inhibits the proliferation, migration, and invasion of tumor cells. Of note, a number of studies have revealed that PTGS2, AKT, and ESR1 are key proteins involved in cancer cell proliferation, migration, and invasion,^{42–44} while p53 and its downstream genes Bcl-2 and Bax play crucial roles in the apoptosis of tumor cells.^{45–47} Importantly, we found that Cur markedly decreases AKT phosphorylation and subsequently inhibits PTGS2 and ESR1 expression, reducing the proliferation, migration, and invasion of colorectal cancer cells. In contrast, Cur induces cancer cell apoptosis by increasing P53 expression and decreasing the Bax/Bcl-2 ratio. Of note, immunotherapy has made significant advances in the treatment of colorectal cancer in recent years, such as targeting immune checkpoints, such as programmed cell death 1 (PD-1) and cytotoxic T lymphocyte antigen 4, chimeric antigen receptor-modified T cells, or cancer vaccines, which have greatly contributed to the development of immunotherapy for colorectal cancer.^{48–50} It has been reported that traditional Chinese medicine, such as Gegen Qinlian decoction⁵¹ and Pien-Tze-Huang,⁵² can enhance the antitumor efficacy of anti-PD-1/PD-L1 immunotherapy. Thus, given that Cur significantly inhibits the growth of colorectal cancer, the synergistic enhancement effect of Cur on immunotherapy deserves further study. In addition, it is also important to explore the effects of isolated compounds on colorectal cancer in vivo. Taken together, these studies suggest that Cur has great therapeutic potential and benefits for colorectal cancer.

CONCLUSIONS

In conclusion, we used molecular docking, in vitro experiments, and a network pharmacology-based approach to confirm the targets of Cur and the potential mechanisms by which its primary active components suppress colorectal cancer effectively. Our results showed that Cur inhibits the development of colorectal cancer by regulating its targets,

which play crucial roles in promoting apoptosis and suppressing cell proliferation, migration, and invasion. This comprehensive approach served as the foundation for the current investigation, which offered a viable alternative therapeutic method with low toxicity that can be used alone or in combination with other medications for the treatment of colorectal cancer.

ASSOCIATED CONTENT

Supporting Information

The Supporting Information is available free of charge at <https://pubs.acs.org/doi/10.1021/acsomega.4c01759>.

The cytotoxicity of Cur to NCM-460 human normal colonic epithelial cells (PDF)

AUTHOR INFORMATION

Corresponding Author

Yi-Ling Jiang – *The First Affiliated Hospital, Department of Oncology, Hengyang Medical School, University of South China, Hengyang, Hunan 421001, China;*
Phone: +8615200500318; Email: 390697964@qq.com

Authors

Zhi-Hui Yin – *The First Affiliated Hospital, Department of Anorectal, Hengyang Medical School, University of South China, Hengyang, Hunan 421001, China;* orcid.org/0009-0005-8785-8871

Wei-Hua Tan – *The First Affiliated Hospital, Emergency Medicine, Hengyang Medical School, University of South China, Hengyang, Hunan 421001, China*

Complete contact information is available at:

<https://pubs.acs.org/10.1021/acsomega.4c01759>

Author Contributions

Y.-L.J. designed and conceived the experiments; Y.-L.J. and Z.-H.Y. wrote the main manuscript text. Z.-H.Y. prepared Figures 1–3, 5–7, 9–14 and helped on the data collection and analysis; W.-H.T. prepared Figures 4 and 8 and helped on the data collection and analysis. The manuscript was reviewed and approved by all authors.

Funding

The authors gratefully acknowledge the Hengyang Science and Technology Board Program (grant/award number. S2018F9031021264.), Scientific Research Project of Health Commission of Hunan Province of China (grant/award number. 202210004450) and the Science and Technology Plan Project of Hengyang City (grant/award number. 2020jh052743).

Notes

The authors declare no competing financial interest.

ACKNOWLEDGMENTS

Not applicable.

REFERENCES

- (1) Patel, S. G.; Karlitz, J. J.; Yen, T.; Lieu, C. H.; Boland, C. R. The rising tide of early-onset colorectal cancer: a comprehensive review of epidemiology, clinical features, biology, risk factors, prevention, and early detection. *Lancet Gastroenterol. Hepatol.* **2022**, *7* (3), 262–274.
- (2) Shin, A. E.; Giancotti, F. G.; Rustgi, A. K. Metastatic colorectal cancer: mechanisms and emerging therapeutics. *Trends Pharmacol. Sci.* **2023**, *44* (4), 222–236.

- (3) Eng, C.; Jácome, A. A.; Agarwal, R.; Hayat, M. H.; Byndloss, M. X.; Holowatyj, A. N.; Bailey, C.; Lieu, C. H. A comprehensive framework for early-onset colorectal cancer research. *Lancet Oncol.* **2022**, *23* (3), e116–e128.
- (4) Morgan, E.; Arnold, M.; Gini, A.; Lorenzoni, V.; Cabasag, C. J.; Laversanne, M.; Vignat, J.; Ferlay, J.; Murphy, N.; Bray, F. Global burden of colorectal cancer in 2020 and 2040: incidence and mortality estimates from GLOBOCAN. *Gut* **2023**, *72* (2), 338–344.
- (5) Dueland, S.; Yaqub, S.; Syversveen, T.; Carling, U.; Hagness, M.; Brudvik, K. W.; Line, P. D. Survival Outcomes After Portal Vein Embolization and Liver Resection Compared With Liver Transplant for Patients With Extensive Colorectal Cancer Liver Metastases. *JAMA Surg.* **2021**, *156* (6), 550–557.
- (6) Morris, V. K.; Kennedy, E. B.; Baxter, N. N.; Benson, A. B., 3rd; Cercek, A.; Cho, M.; Ciombor, K. K.; Cremolini, C.; Davis, A.; Deming, D. A.; Fakih, M. G.; Gholami, S.; Hong, T. S.; Jaiyesimi, I.; Klute, K.; Lieu, C.; Sanoff, H.; Strickler, J. H.; White, S.; Willis, J. A.; Eng, C. Treatment of Metastatic Colorectal Cancer: ASCO Guideline. *J. Clin. Oncol.* **2023**, *41* (3), 678–700.
- (7) Cervantes, A.; Adam, R.; Roselló, S.; Arnold, D.; Normanno, N.; Taïeb, J.; Seligmann, J.; De Baere, T.; Osterlund, P.; Yoshino, T.; Martinelli, E. Metastatic colorectal cancer: ESMO Clinical Practice Guideline for diagnosis, treatment and follow-up. *Ann. Oncol.* **2023**, *34* (1), 10–32.
- (8) Ganesh, K.; Stadler, Z. K.; Cercek, A.; Mendelsohn, R. B.; Shia, J.; Segal, N. H.; Diaz, L. A. Immunotherapy in colorectal cancer: rationale, challenges and potential. *Nat. Rev. Gastroenterol Hepatol* **2019**, *16* (6), 361–375.
- (9) Ganesh, K. Optimizing immunotherapy for colorectal cancer. *Nat. Rev. Gastroenterol Hepatol* **2022**, *19* (2), 93–94.
- (10) Agarwal, P.; Le, D. T.; Boland, P. M. Immunotherapy in colorectal cancer. *Adv. Cancer Res.* **2021**, *151*, 137–196.
- (11) Wu, Y. Y.; Xu, Y. M.; Lau, A. T. Y. Epigenetic effects of herbal medicine. *Clin. Epigenet.* **2023**, *15* (1), 85.
- (12) Li, Z.; Feiyue, Z.; Gaofeng, L. Traditional Chinese medicine and lung cancer-From theory to practice. *Biomed. Pharmacother.* **2021**, *137*, 111381.
- (13) Shang, L.; Wang, Y.; Li, J.; Zhou, F.; Xiao, K.; Liu, Y.; Zhang, M.; Wang, S.; Yang, S. Mechanism of Sijunzi Decoction in the treatment of colorectal cancer based on network pharmacology and experimental validation. *J. Ethnopharmacol.* **2023**, *302* (Pt A), 115876.
- (14) Bu, F.; Tu, Y.; Wan, Z.; Tu, S. Herbal medicine and its impact on the gut microbiota in colorectal cancer. *Front. Cell. Infect. Microbiol.* **2023**, *13*, 1096008.
- (15) Albaqami, J. J.; Hamdi, H.; Narayanankutty, A.; Visakh, N. U.; Sasidharan, A.; Kuttithodi, A. M.; Famurewa, A. C.; Pathrose, B. Chemical Composition and Biological Activities of the Leaf Essential Oils of *Curcuma longa*, *Curcuma aromatica* and *Curcuma angustifolia*. *Antibiotics* **2022**, *11* (11), 1547.
- (16) Fei, C.; Ji, D.; Tong, H.; Li, Y.; Su, L.; Qin, Y.; Bian, Z.; Zhang, W.; Mao, C.; Li, L.; Lu, T. Therapeutic mechanism of *Curcuma aromatica* Salisb. rhizome against coronary heart disease based on integrated network pharmacology, pharmacological evaluation and lipidomics. *Front. Pharmacol.* **2022**, *13*, 950749.
- (17) Liu, F.; Liang, Y.; Sun, R.; Yang, W.; Liang, Z.; Gu, J.; Zhao, F.; Tang, D. *Astragalus mongholicus* Bunge and *Curcuma aromatica* Salisb. inhibits liver metastasis of colon cancer by regulating EMT via the CXCL8/CXCR2 axis and PI3K/AKT/mTOR signaling pathway. *Chin. Med.* **2022**, *17* (1), 91.
- (18) Li, Y.; Wo, J. M.; Liu, Q.; Li, X.; Martin, R. C. Chemoprotective effects of *Curcuma aromatica* on esophageal carcinogenesis. *Ann. Surg. Oncol.* **2009**, *16* (2), 515–523.
- (19) Du, Q.; Hu, B.; An, H. M.; Shen, K. P.; Xu, L.; Deng, S.; Wei, M. M. Synergistic anticancer effects of curcumin and resveratrol in Hepa1–6 hepatocellular carcinoma cells. *Oncol. Rep.* **2013**, *29* (5), 1851–1858.
- (20) Gu, J.; Sun, R.; Wang, Q.; Liu, F.; Tang, D.; Chang, X. Standardized *Astragalus Mongholicus* Bunge-*Curcuma Aromatica* Salisb. Extract Efficiently Suppresses Colon Cancer Progression Through Gut Microbiota Modification in CT26-Bearing Mice. *Front. Pharmacol.* **2021**, *12*, 714322.
- (21) Kim, H.; Hong, J.; Lee, J.; Jeon, W.; Yeo, C.; Lee, Y.; Baek, S.; Ha, I. *Curcuma aromatica* Salisb. Protects from Acetaminophen-Induced Hepatotoxicity by Regulating the Sirt1/HO-1 Signaling Pathway. *Nutrients* **2023**, *15* (4), 808.
- (22) Li, Y.; Shi, X.; Zhang, J.; Zhang, X.; Martin, R. C. Hepatic protection and anticancer activity of curcuma: a potential chemopreventive strategy against hepatocellular carcinoma. *Int. J. Oncol.* **2014**, *44* (2), 505–513.
- (23) Zhu, W.; Zhang, R.; Ma, C.; Hu, Y.; Shi, X.; Wang, X.; Wu, X.; Ai, K. Study on the Action Mechanism of the Yifei Jianpi Tongfu Formula in Treatment of Colorectal Cancer Lung Metastasis Based on Network Analysis, Molecular Docking, and Experimental Validation. *Evidence-Based Complementary and Alternative Medicine; Hindawi*, 2022; Vol. 2022, pp 1–14.
- (24) Ericson, K.; Gan, C.; Cheong, I.; Rago, C.; Samuels, Y.; Velculescu, V. E.; Kinzler, K. W.; Huso, D. L.; Vogelstein, B.; Papadopoulos, N. Genetic inactivation of AKT1, AKT2, and PDPK1 in human colorectal cancer cells clarifies their roles in tumor growth regulation. *Proc. Natl. Acad. Sci. U.S.A.* **2010**, *107* (6), 2598–2603.
- (25) Belshaw, N. J.; Elliott, G. O.; Williams, E. A.; Mathers, J. C.; Buckley, L.; Bahari, B.; Johnson, I. T. Methylation of the ESR1 CpG island in the colorectal mucosa is an “all or nothing” process in healthy human colon, and is accelerated by dietary folate supplementation in the mouse. *Biochem. Soc. Trans.* **2005**, *33* (4), 709–711.
- (26) Venè, R.; Costa, D.; Augugliaro, R.; Carlone, S.; Scabini, S.; Casoni Pattacini, G.; Boggio, M.; Zupo, S.; Grillo, F.; Mastracci, L.; Pitto, F.; Minghelli, S.; Ferrari, N.; Tosetti, F.; Romairone, E.; Mingari, M. C.; Poggi, A.; Benelli, R. Evaluation of Glycosylated PTGS2 in Colorectal Cancer for NSAIDS-Based Adjuvant Therapy. *Cells* **2020**, *9* (3), 683.
- (27) Meng, J.; Wang, L.; Hou, J.; Yang, X.; Lin, K.; Nan, H.; Li, M.; Wu, X.; Chen, X. CCL23 suppresses liver cancer progression through the CCR1/AKT/ESR1 feedback loop. *Cancer Sci.* **2021**, *112* (8), 3099–3110.
- (28) St-Germain, M. E.; Gagnon, V.; Mathieu, I.; Parent, S.; Asselin, E. Akt regulates COX-2 mRNA and protein expression in mutated-PTEN human endometrial cancer cells. *Int. J. Oncol.* **2004**, *24* (5), 1311–1324.
- (29) Liu, T.; Lam, V.; Thieme, E.; Sun, D.; Wang, X.; Xu, F.; Wang, L.; Danilova, O. V.; Xia, Z.; Tyner, J. W.; Kurtz, S. E.; Danilov, A. V. Pharmacologic Targeting of Mcl-1 Induces Mitochondrial Dysfunction and Apoptosis in B-Cell Lymphoma Cells in a TP53- and BAX-Dependent Manner. *Clin. Cancer Res.* **2021**, *27* (17), 4910–4922.
- (30) Flórez, M. M.; Fêo, H. B.; da Silva, G. N.; Yamatogi, R. S.; Aguiar, A. J.; Araújo, J. P., Jr; Rocha, N. S. Cell cycle kinetics, apoptosis rates and gene expressions of MDR-1, TP53, BCL-2 and BAX in transmissible venereal tumour cells and their association with therapy response. *Vet. Comp. Oncol.* **2017**, *15* (3), 793–807.
- (31) Luo, Y.; Fu, X.; Ru, R.; Han, B.; Zhang, F.; Yuan, L.; Men, H.; Zhang, S.; Tian, S.; Dong, B.; Meng, M. CpG Oligodeoxynucleotides Induces Apoptosis of Human Bladder Cancer Cells via Caspase-3-Bax/Bcl-2-p53 Axis. *Arch. Med. Res.* **2020**, *51* (3), 233–244.
- (32) Qiu, W.; Leibowitz, B.; Zhang, L.; Yu, J. Growth factors protect intestinal stem cells from radiation-induced apoptosis by suppressing PUMA through the PI3K/AKT/p53 axis. *Oncogene* **2010**, *29* (11), 1622–1632.
- (33) Qi, D.; Song, X.; Xue, C.; Yao, W.; Shen, P.; Yu, H.; Zhang, Z. AKT1/FOXp3 axis-mediated expression of CerS6 promotes p53 mutant pancreatic tumorigenesis. *Cancer Lett.* **2021**, *522*, 105–118.
- (34) Dekker, E.; Tanis, P. J.; Vleugels, J. L. A.; Kasi, P. M.; Wallace, M. B. Colorectal cancer. *Lancet* **2019**, *394* (10207), 1467–1480.
- (35) Noor, F.; Tahir Ul Qamar, M.; Ashfaq, U. A.; Albutti, A.; Alwashmi, A. S. S.; Aljasir, M. A. Network Pharmacology Approach for Medicinal Plants: Review and Assessment. *Pharmaceuticals (Basel)* **2022**, *15* (5), 572.

- (36) Sharma, B.; Yadav, D. K. Metabolomics and Network Pharmacology in the Exploration of the Multi-Targeted Therapeutic Approach of Traditional Medicinal Plants. *Plants (Basel)* **2022**, *11* (23), 3243.
- (37) Leem, J.; Jung, W.; Park, H. J.; Kim, K. A network pharmacology-based approach to explore mechanism of action of medicinal herbs for alopecia treatment. *Sci. Rep.* **2022**, *12* (1), 2852.
- (38) Gao, F.; Niu, Y.; Sun, L.; Li, W.; Xia, H.; Zhang, Y.; Geng, S.; Guo, Z.; Lin, H.; Du, G. Integrating network pharmacology and transcriptomic validation to investigate the efficacy and mechanism of Mufangji decoction preventing lung cancer. *J. Ethnopharmacol.* **2022**, *298*, 115573.
- (39) Gao, J.; Yang, S.; Xie, G.; Pan, J.; Zhu, F. Integrating Network Pharmacology and Experimental Verification to Explore the Pharmacological Mechanisms of Aloin Against Gastric Cancer. *Drug Des. Dev. Ther.* **2022**, *16*, 1947–1961.
- (40) Hu, B.; Shen, K. P.; An, H. M.; Wu, Y.; Du, Q. Aqueous extract of *Curcuma aromatica* induces apoptosis and G2/M arrest in human colon carcinoma LS-174-T cells independent of p53. *Cancer Biother. Rad.* **2011**, *26* (1), 97–104.
- (41) Panich, U.; Kongtaphan, K.; Onkoksoong, T.; Jaemsak, K.; Phadungrakwittaya, R.; Thaworn, A.; Akarasereenont, P.; Wongkajornsilp, A. Modulation of antioxidant defense by *Alpinia galanga* and *Curcuma aromatica* extracts correlates with their inhibition of UVA-induced melanogenesis. *Cell Biol. Toxicol.* **2010**, *26* (2), 103–116.
- (42) Zeng, Q.; Nie, X.; Li, L.; Liu, H. F.; Peng, Y. Y.; Zhou, W. T.; Hu, X. J.; Xu, X. Y.; Chen, X. L. Solidroside Promotes Sensitization to Doxorubicin in Human Cancer Cells by Affecting the PI3K/Akt/HIF Signal Pathway and Inhibiting the Expression of Tumor-Resistance-Related Proteins. *J. Nat. Prod.* **2022**, *85* (1), 196–204.
- (43) Wang, L.; Cui, M.; Cheng, D.; Qu, F.; Yu, J.; Wei, Y.; Cheng, L.; Wu, X.; Liu, X. miR-9-5p facilitates hepatocellular carcinoma cell proliferation, migration and invasion by targeting ESR1. *Mol. Cell. Biochem.* **2021**, *476* (2), 575–583.
- (44) Cai, B.; Qu, X.; Kan, D.; Luo, Y. miR-26a-5p suppresses nasopharyngeal carcinoma progression by inhibiting PTGS2 expression. *Cell Cycle* **2022**, *21* (6), 618–629.
- (45) Moradipour, A.; Dariushnejad, H.; Ahmadzadeh, C.; Lashgarian, H. E. Dietary flavonoid carvacrol triggers the apoptosis of human breast cancer MCF-7 cells via the p53/Bax/Bcl-2 axis. *Med. Oncol.* **2022**, *40* (1), 46.
- (46) Kandhavelu, J.; Subramanian, K.; Naidoo, V.; Sebastianelli, G.; Doan, P.; Konda Mani, S.; Yapislari, H.; Haciosmanoglu, E.; Arslan, L.; Ozer, S.; Thiyyagarajan, R.; Candeias, N. R.; Penny, C.; Kandhavelu, M.; Murugesan, A. A novel EGFR inhibitor, HNPML, regulates apoptosis and oncogenesis by modulating BCL-2/BAX and p53 in colon cancer. *Br. J. Pharmacol.* **2024**, *181* (1), 107–124.
- (47) Wei, H.; Wang, H.; Wang, G.; Qu, L.; Jiang, L.; Dai, S.; Chen, X.; Zhang, Y.; Chen, Z.; Li, Y.; Guo, M.; Chen, Y. Structures of p53/BCL-2 complex suggest a mechanism for p53 to antagonize BCL-2 activity. *Nat. Commun.* **2023**, *14* (1), 4300.
- (48) Johdi, N. A.; Sukor, N. F. Colorectal Cancer Immunotherapy: Options and Strategies. *Front. Immunol.* **2020**, *11*, 1624.
- (49) Fan, A.; Wang, B.; Wang, X.; Nie, Y.; Fan, D.; Zhao, X.; Lu, Y. Immunotherapy in colorectal cancer: current achievements and future perspective. *Int. J. Biol. Sci.* **2021**, *17* (14), 3837–3849.
- (50) Zhao, W.; Jin, L.; Chen, P.; Li, D.; Gao, W.; Dong, G. Colorectal cancer immunotherapy-Recent progress and future directions. *Cancer Lett.* **2022**, *545*, 215816.
- (51) Lv, J.; Jia, Y.; Li, J.; Kuai, W.; Li, Y.; Guo, F.; Xu, X.; Zhao, Z.; Lv, J.; Li, Z. Gegen Qinlian decoction enhances the effect of PD-1 blockade in colorectal cancer with microsatellite stability by remodelling the gut microbiota and the tumour microenvironment. *Cell Death Dis.* **2019**, *10* (6), 415.
- (52) Chen, Q.; Hong, Y.; Weng, S.; Guo, P.; Li, B.; Zhang, Y.; Yu, C.; Wang, S.; Mo, P. Traditional Chinese Medicine Pien-Tze-Huang Inhibits Colorectal Cancer Growth and Immune Evasion by Reducing β -catenin Transcriptional Activity and PD-L1 Expression. *Front. Pharmacol.* **2022**, *13*, 828440.